Two-pore channel 1 interacts with citron kinase, regulating completion of cytokinesis

Jaime S Horton[1,2], Clay T Wakano[3], Mark Speck[4], and Alexander J Stokes[1,2,4,*]

[1]Laboratory of Experimental Medicine; John A. Burns School of Medicine; University of Hawaii; Honolulu, HI USA; [2]Department of Cell and Molecular Biology; John A. Burns School of Medicine; University of Hawaii; Honolulu, HI USA; [3]Queens Center for Biomedical Research; Honolulu, HI USA; [4]Chaminade University; Honolulu, HI USA

Two-pore channels (TPC1, 2, and 3) are recently identified endolysosomal ion channels, but remain poorly characterized. In this study, we show for the first time a role for TPC1 in cytokinesis, the final step in cell division. HEK 293 T-REx cells inducibly overexpressing TPC1 demonstrated a lack of proliferation accompanied by multinucleation and an increase in G2/M cycling cells. Increased TPC1 was associated with a concomitant accumulation of active RhoGTP and a decrease in phosphorylated myosin light chain (MLC). Finally, we demonstrated a novel interaction between TPC1 and citron kinase (CIT). These results identify TPC1 as a central component of cytokinetic control, specifically during abscission, and introduce a means by which the endolysosomal system may play an active role in this process.

Introduction

The 2-pore channels (TPC1, 2 and 3) constitute a family of endolysosomal ion channels, and belong to the 6 transmembrane (6TM) ion channel superfamily with homology to voltage-gated ion channels. Unlike plasma membrane Na_V and Ca_V channels, the primary structures of TPCs contain 2, instead of 4, 6TM domains,[1] each containing a pore-forming loop, suggesting that TPCs represent an evolutionary intermediate between single 6TM and 4 6TM channels.[2,3] TPCs are encoded by 3 genes in most deuterostomes, including sea urchins, whereas only 2 isoforms, TPC1 and TPC2, are present in rats, mice and humans.[3-5] TPC transcripts are found in most human and mouse tissues, suggesting a ubiquitous function.[3,6] All TPC isoforms localize to acidic organelles, with TPC2 expression predominantly lysosomal, and TPC1 with a wider distribution within the endolysosomal system, found in lysosomes, early and recycling endosomes.[3,4,7]

In plants, studies of Ca^{2+} release in Arabidopsis identified AtTPC1 as a channel[8] that mediates the slow vacuolar current,[9] regulating germination and stomatal movement.[10] TPCs have been shown to regulate differentiation,[11] smooth muscle contraction[12] and endothelial cell activation,[13] consistent with previous studies implicating nicotinic acid adenine dinucleotide phosphate (NAADP)-induced Ca^{2+} release in these events,[14-16] and supported by several overexpression, knockdown and knockout models.[3,4,6,17] Regulation and affinity of TPC ion channels is a contentious issue. Literature suggest proton-permeable ion channels activated by NAADP or Ca^{2+};[18] although photoaffinity labeling studies suggest that NAADP does not directly bind TPCs.[19,20] However other studies indicate Na^+-selective channels regulated by phosphoinositide-3,5-bisphosphate $(PI(3,5)P_2)$ and ATP.[21,22] Further studies may still be needed to account for both sets of data.

Our data show a role for TPC channels in cytokinesis, the final step in cell division. This is a highly ordered process, requiring an intricate interplay between cytoskeletal, chromosomal and cell cycle regulatory pathways. A number of additional cellular processes are also important in cytokinesis, including protein and membrane trafficking, lipid metabolism, protein synthesis and DNA damage.[23] Dys-regulation of this process can cause multinucleation and aneuploidy, processes that can lead to chromosomal instability and directly impact cancer progression.[24-26] Successful partitioning of cytoplasmic and genomic materials at the end of cell division requires a transition from constriction to abscission and interaction between contractile ring and spindle components, but how these events are coordinated is not well understood.

In the present study, we show that overexpression of TPC1, but not TPC2, causes the cessation of cellular proliferation associated with multinucleation and abnormal cell cycle distribution. TPC1 was shown to interact with citron kinase (CIT), with TPC1 overexpression affecting RhoA activity and myosin light chain (MLC) phosphorylation levels in cytokinesis. These results indicate an important role for the endolysosomal system in cell cycle regulation.

Materials and Methods

Plasmid constructs

C-terminal FLAG-tagged human TPC1 and TPC2 clones were obtained from Open BioSystems, pCAG plasmid harboring a myc-tagged CIT fusion protein was a gift from Dr. Narumiya at Kyoto University, and RhoA clones were obtained from the University of Missouri-Rolla cDNA Resource Center. TPC target cDNAs were PCR-amplified to include a FLAG tag epitope and cloned into pcDNA4/TO or pcDNA5/TO vectors (Life Technologies). Site-directed mutagenesis was performed with the QuikChange II XL kit (Stratagene) according to the manufacturer's instructions.

Cell culture and transfection

HEK 293 T-REx cells (Life Technologies) were maintained in DMEM and 10% fetal bovine serum supplemented with 2 mM glutamine, and maintained in a humidified atmosphere of 5% CO_2 at 37°C. Tetracycline-inducible stable cell lines were generated by electroporation and maintained in media supplemented with selective compounds zeocin or blasticidin and hygromycin. Positive clones were screened by co-immunoprecipitation and western blotting. Induction was induced by 1 μg/ml tetracycline for 16 h. Cells were synchronized by serum starvation (0% FBS) for 48 h before use. Transient transfection of HEK 293 T-REx cells with the pCAG plasmid was achieved with TransIT transfection reagent (Mirus Bio).

Proliferation assay

Cells were harvested at various time points and lysed on ice in buffer (50 mM HEPES pH 7.4, 75 mM NaCl, 20 mM NaF, 10 mM iodoacetmide, 0.5% Triton X-100, 1 mM PMSF and protease cocktail inhibitor). Total protein was measured from 5 μl of lysate with the DC Protein Assay (Bio-Rad) and performed in triplicate.

Transmission electron microscopy

Cells were fixed with 2% PFA and glutaraldehyde in 0.1 M phosphate buffer, pH 7.4 for 20 min at RT. Cells were washed twice in 0.1 M cacodylate buffer for 5 min, and postfixed with 1% OsO4 in 0.1 M cacodylate buffer for 1 hour. En-bloc staining was performed in 1% aqueous uranyl acetate for 30 min, then cells were dehydrated in a graded ethanol series (30%, 50%, 70%, 85%, 95%, 100%), substituted with propylene oxide, and embedded in LX112 epoxy resin. After epoxy resin infiltration, samples were placed in molds and polymerized at 60°C for 2 days. Ultrathin (60–80 nm) sections were obtained on a Reichert Ultracut E ultramicrotome, double stained with uranyl acetate and lead citrate, viewed on a LEO/Zeiss 912 EFTEM at 100 kV, and photographed with a Proscan frame-transfer CCD.

Immunofluorescence microscopy

HEK 293 T-REx cells were grown on cover slips and fixed with methanol for 10 min at −20°C. After blocking in 0.7% fish skin gelatin (FSG) in PBS, cells were incubated with rabbit anti-TPC1 (Bethyl Labs, 1 μg/ml in 0.05% FSG) and mouse anti-CIT (BD, 0.5 μg/ml in 0.05% FSG), washed, and incubated with anti-mouse Alexa488 and anti-rabbit Alexa568 secondary antibodies (Life Technologies, 0.5 μg/ml in 0.05% FSG) and washed. Nuclei were counterstained with Hoechst 33342 (100 μg/ml) for 5 min at RT. Cells were imaged on an Olympus IX70 fluorescence inverted microscope with quadruple dichroic filter block and excitation filter set 88000 (Chroma), connected to an F-view monochrome CCD camera.

Flow cytometry

Cells were washed in buffer (PBS, 2% FBS) and spun at 1000 rpm for 5 min, resuspended in buffer, and fixed in 75% ethanol for 1 h at 4°C. Cells were washed twice in buffer and stained with propidium iodide in the presence of RNAse A for 30 min at 37°C. Analysis was performed on a Beckman Coulter EPICS Elite EPS Flow Cytometer. Data was analyzed with FloJo software (Treestar).

Mass spectrometry

Liquid chromatography mass spectrometry (LC/MS) analysis was performed by the W.M. KECK Foundation Biotechnology Resource Laboratory at Yale University. Samples were resolved on a 2-D PAGE gel, stained with coomassie blue, and in-gel trypsin digestion performed on bands of interest. Analysis was performed on a Micromass Q-TOF API mass spectrometer, with chromatographic separation performed on a C18 analytical column (100 μm i.d., Atlantis). Proteins were identified from spectra with the Mascot Distiller and Mascot database search algorithm (Matrix Science).

Co-immunoprecipitation (Co-IP)

Cells were lysed as previously described, cleared by centrifugation and incubated with anti-FLAG M2 (Sigma-Aldrich) or c-myc (Abgent) for 1.5 h at 4°C. Antibody complexes were captured onto protein A agarose beads (Sigma Aldrich), recovered at 12,000 rpm for 1 min and subjected to 2–4 washes with lysis buffer. Immunoprecipitated proteins were eluted with reducing sample buffer (20% glycerol, 62.5 mM Tris-HCl pH 6.8, 0.05% bromophenol blue, 2 mM 2-mercaptoethanol) and boiled at 95°C for 8 min. Total protein was acetone precipitated and solubilized in reducing sample buffer.

Western blotting

Total protein and immunoprecipitated samples were resolved by SDS-PAGE and transferred to PVDF membrane, blocked with 5% non-fat milk or BSA for 1 h at RT and incubated overnight at 4°C with primary antibody (TPC1 and TPC2, Bethyl Laboratories; cyclin B1, phospho-cdc2, phospho-Rb, cyclin E1, cyclin A, phospho-p44/42 MAPK, phospho-MLC2, Cell Signaling Technology) diluted in antibody diluent (15 mM Tris base, 150 mM NaCl, 0.05% Tween-20, 0.05% NaN$_3$). The membrane was washed in TTBS (15 mM Tris base, 150 mM NaCl, 0.05% Tween-20) and incubated with HRP-conjugated IgG antibodies (GE Healthcare, 1:12,000) in 0.5% non-fat milk at RT for 45 min before visualization with ECL Plus detection reagent (GE Healthcare) on a Kodak X-OMAT 2000A processor

with Kodak X-OMAT LS imaging film. Densitometry analysis was performed using ImageJ software.

Human tumor array

Human tumor tissue array (Biochain), was blocked with 5% non-fat milk or BSA for 1 h at RT and incubated overnight at 4°C with primary antibody (TPC1, Bethyl Laboratories) diluted in antibody diluent (15 mM Tris base, 150 mM NaCl, 0.05% Tween-20, 0.05% NaN$_3$). The membrane was washed in TTBS (15 mM Tris base, 150 mM NaCl, 0.05% Tween-20) and incubated with HRP-conjugated IgG antibodies (GE Healthcare, 1:12,000) in 0.5% non-fat milk at RT for 45 min before visualization with ECL Plus detection reagent (GE Healthcare) on a Kodak X-OMAT 2000A processor with Kodak X-OMAT LS imaging film. Densitometry analysis was performed using the Dot_Blot_Analyzer macro in the Fiji release of ImageJ (imagej.nih.gov/ij/).

Rho GTPase activation assay

Cells were lysed on ice in 25 mM HEPES pH 7.5, 150 mM NaCl, 1% NP-40, 10% glycerol, 25 mM NaF, 1 mM EDTA, 1 mM PMSF and 1 mM sodium orthovanadate. Lysates were cleared by centrifugation at 14,000 × g for 5 min at 4°C, and loaded with 10 mM 0.5 M EDTA and 100 uM GTPγS (Sigma) or 1 mM GDP (Sigma) for 30 min at 30°C. Lysates were incubated with 20 μg Rhotekin-RBD agarose (Upstate) for 45 min at 4°C, recovered by centrifugation at 14,000 × g for 10 s at 4°C and washed 3 times with lysis buffer. Samples were incubated at 95°C for 8 min in sample buffer containing 1 M DTT and resolved by SDS-PAGE.

Statistical analyses

Tissue array analyses were carried out with R, a free software environment available at http://www.r-project.org/. Box plots were drawn using the ggplot2 and reshape2 packages following routines originally developed by Tukey. Volcano plots were generated from –log$_{10}$ values from unpaired Student's t-test vs. the average ratio fold change of the tumor to the normal tissue observations, and drawn with the plotrix package. Unless otherwise indicated, all data is shown as mean ± SEM of 3 replicates.

Results

Overexpression of TPC1, but not TPC2, causes cessation of cellular proliferation

HEK 293 T-REx cells induced with tetracycline to overexpress TPC1 or TPC2 were grown over a period of 5 days. TPC1, but not TPC2 cells, demonstrated a decrease in cellular proliferation as measured by total protein content over time (**Fig. 1A**). This reduction in cell proliferation was apparent by 48 h, and maintained thru day 5. Phenotypically, TPC1-overexpressing cells showed a characteristic rounding of cells in chains or clusters, progressing to detachment from the substrate that was not a result of apoptosis (data not shown). Instead, a possible defect in cellular division was investigated.

TPC1 overexpression causes multinucleation and abnormal cell cycle distribution

Transmission electron microscope (TEM) images of TPC1 cells after 72 h of growth showed enlargement and multinucleation of cells compared to wild-type (WT) HEK 293 T-REx cells (**Fig. 1B**). Mixed population experiments indicated that multinucleation was not a result of cell fusion (data not shown). TPC1 cells formed multiple membrane-enclosed nuclei, indicating mitotic failure rather than cell cycle arrest. To confirm this, flow cytometric analysis of DNA content was measured over a period of 96 h. TPC1 over-expressing cells showed marked G2/M accumulation and appearance of greater than tetraploid (>4 N) populations compared to WT cells (**Fig. 1C**), suggesting that TPC1 overexpression is associated with abnormal cell cycle regulation, resulting in polyploidy. Removing and rinsing the tetracycline containing media from the cells after 24 hours did not rescue them from the cell cycle disruption and multinucleation (data not shown).

TPC1 and TPC2 protein levels are modulated during the cell cycle

Due to their possible role(s) in cell cycle regulation, TPC1 and TPC2 expression was compared to that of various cell cycle markers. WT cells were synchronized by serum starvation and analyzed for endogenous TPC1 or TPC2 expression by Western blot. Endogenous TPC1 and TPC2 protein levels fluctuated over time, similar to the cycling expression patterns of phospho-cdc2, cyclin A, cyclin B1, phospho-Rb and cyclin E1 (**Fig. 2**). Specifically, TPC1 expression appears to peak at the G2/M transition, whereas TPC2 levels are highest between the S and G2 phases.

TPC1 interacts with citron kinase

To further elucidate the role of TPC1 in cell cycle regulation, TPC1 binding partners were investigated. LC/MS/MS analysis of TPC1-interacting proteins identified citron kinase (CIT) as an N-terminus binding partner of TPC1 (data not shown). CIT acts as a key facilitator of late events during cytokinesis, by regulating a molecular network of contractile ring components and microtubule-associated proteins.[27] This interaction was confirmed by co-immunoprecipitation of TPC1-FLAG-overexpressing cells transiently transfected with CIT-myc (**Fig. 3A**). Observing this interaction between TPC1 and CIT, we sought to determine the subcellular localization of the TPC1-CIT complex through the cell cycle. In non-dividing cells, TPC1 and CIT were localized diffusely throughout the cell, but during mitosis, TPC1 and CIT appeared to colocalize in membrane areas surrounding separating chromatids (**Fig. 3B**). Thus the spatial distribution of TPC1 may be specially coordinated to enable its participation in cytokinesis.

TPC1 overexpression results in the accumulation of active RhoGTP and reduced pMLC

The small GTPase RhoA is a central component of cytokinesis control in eukaryotes, controlling actin polymerization during formation and stabilization of the cleavage furrow, and also drives
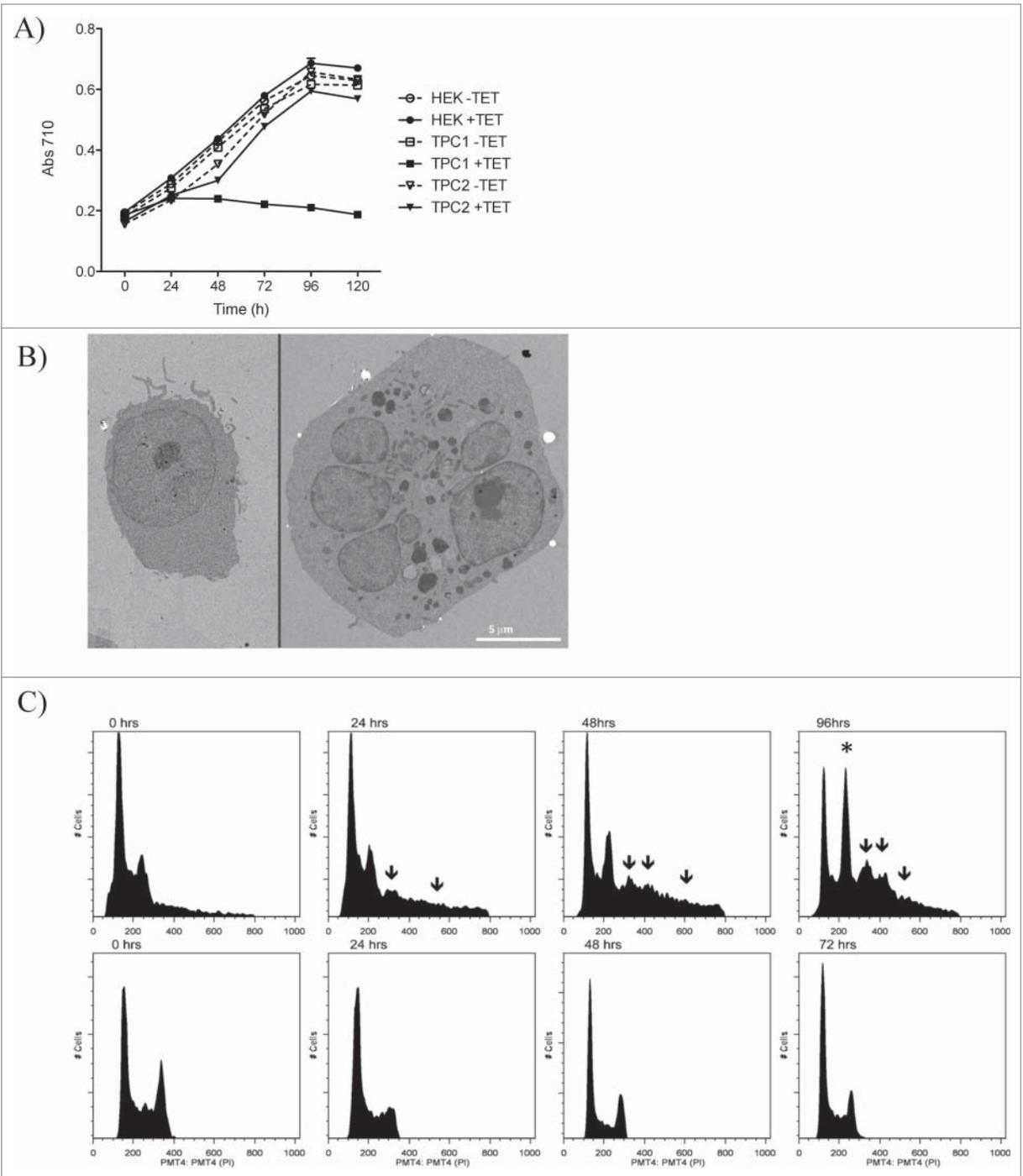
Figure 1. Overexpression of TPC1, but not TPC2, causes cessation of cellular proliferation and multinucleation. (**A**) Growth analysis of HEK 293 T-REx cells overexpressing TPC1 or TPC2 induced by tetracycline. Cellular growth based on total protein content measured with the DC protein assay (Bio Rad). Samples were analyzed in triplicate. (**B**) Representative electron microscope image of wild-type HEK 293 T-REx cells (left) and cells overexpressing TPC1 (right) after 72 h of growth. Scale bar = 5 μm. (**C**) DNA content of HEK 293 T-REx cells overexpressing TPC1 (top panel) compared to wild-type cells (bottom panel) over 96 h. TPC1 expression was induced by tetracycline treatment, and DNA content assessed by propidium iodide staining by flow cytometry. Increased G2/M accumulation indicated by*. The appearance of >4 N populations are indicated by arrows.

contraction of the actin ring through myosin light chain (MLC) phosphorylation.[28,29] Since CIT is essential to maintaining proper RhoA localization at the cleavage site during cytokinesis,[30,31] we sought to determine the effect of TPC1 overexpression on RhoA activation and MLC phosphorylation. Using a RhoGTP affinity assay, levels of active RhoGTP were shown to increase with TPC1 overexpression over time (**Fig. 4A**). Concomitant with TPC1 induction, phospho-p44/42
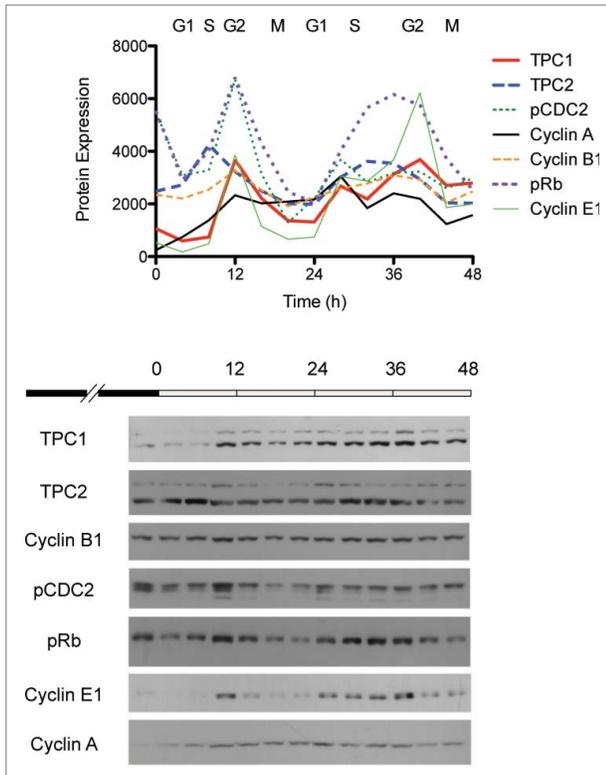
Figure 2. Correlation of endogenous TPC1 and TPC2 expression with cell cycle markers in HEK 293 T-REx cells. Wild-type cells were synchronized by serum starvation for 48 h and analyzed at 4 h intervals by Western blot. Protein expression was quantitated by densitometric analysis and plotted over time. Lower panel, representative Western blot of synchronized HEK 293 T-REx cells probed for TPC1, TPC2 and several cell cycle markers.

MAPK expression increased while phospho-MLC2 levels decreased (**Fig. 4B**). These results indicate that overexpression of TPC1 may sequester CIT, restraining RhoGTP localization and MLC phosphorylation, and inhibiting actin ring contractility and abscission.

Overexpression of WT RhoA, a dominant-negative mutant of RhoA, or a constitutively active RhoA mutant, was unable to overcome the proliferation defect induced by TPC1 overexpression (**Suppl. Fig. 1**).

TPC1 is upregulated in human tumor tissues

Deregulation of the cell cycle, and specifically, cytokinesis failure, directly contributes to genetic instability and the development of cancer cells.[32] Since cytokinetic defects and multinucleation were observed in TPC1-overexpressing cells, we measured TPC1 protein expression in an array of human tumor tissues. Compared to normal tissues, tumor tissues expressed significantly more TPC1 (**Fig. 5**). Furthermore, the ratio fold-change of tumor to normal tissue TPC1 expression was statistically significant for the vast majority of tissue types examined (**Suppl. Fig. 2**), further highlighting a link between TPC1 dysregulation and tumorigenicity.

Discussion

We show here a novel role for TPC1 in cell cycle regulation, specifically, in the initiation of the cleavage furrow needed to achieve cytokinesis. Cells overexpressing TPC1 were shown to have a proliferation defect, accompanied by a multinucleation phenotype and polyploidy. TPC1 overexpression was also associated with increased RhoGTP levels and decreased MLC phosphorylation. Moreover, we present evidence for a novel protein-protein interaction between TPC1 and CIT, which could cause the disruption in MLC phosphorylation and cytokinesis that we observe.

The connection between cell cycle completion and CIT has been well-established, with CIT knockout or siRNA knockdown experiments showing an increase in tetraploid/multinucleate cells and cytokinetic defects.[33-37] It was initially proposed that mammalian CIT acted during cleavage furrow ingression, regulating the levels of di-phosphorylated MLC downstream of RhoA.[38-40] However, more recent studies suggest that CIT is specifically involved in the latest stages of cytokinesis, during abscission,[41,42] not as a RhoA effector, but instead to maintain proper RhoA localization at the cleavage site during cytokinesis.[30,31] CIT has been postulated to be a scaffold protein,[30,43] and indeed, its multi-domain structure has been shown to bind with ROCK II, profilin IIa, LIMK, p116RIP, anillin, Dlg5,[30,44,45] and other mitotic proteins including PRC1, KIF14, RanBPM and Plk1.[41,46,47] Most recently, p27Kip1 was shown to compete with RhoA for binding to CIT, causing multinucleation and polyploidy.[43] We propose that multinucleation in TPC1-overexpressing cells may similarly be a result of sequestration or competitive binding between TPC1 and CIT. We found TPC1 overexpression to be associated with an accumulation of active RhoA. Temporal and spatial regulation of active RhoA is necessary for successful cytokinesis completion,[30,48] therefore our data support that TPC1 sequestration of CIT and disruption of the appropriate CIT-RhoA interaction results in compensation with the production of excess RhoGTP. In an attempt to rescue the multinucleation caused by over-expression of TPC1, we overexpressed CIT but did not overcome the proliferation defect (data not shown). We propose that once cell cycle dysregulation occurs past expected mitosis there is no capacity for reversion, as it would be hard to imagine the accurate organization of division machinery in >3 n ploidy cell allowing cytokinesis into more than 2 cells simultaneously. Other published CIT overexpression studies also showed abscission delay,[30] suggesting that dysregulation of CIT activity in general is capable of effecting cytokinetic defects.

TPC1 overexpression was also associated with a decrease in MLC phosphorylation (**Fig. 4B**). In eukaryotes, phosphorylation of the regulatory light chain of myosin II, the principal motor responsible for cytokinesis, is a primary means of its activation.[40] While studies performed in both drosophila[49] and mammalian cells[40] indicate that CIT has little or no role in regulating MLC phosphorylation in vivo, analysis of myosin phosphorylation in CIT knockout mice revealed that pMLC was increased, rather than decreased, in the neuronal precursors of mutant mice.[40]

Thus TPC1-mediated decreases in MLC phosphorylation are likely to be CIT-independent. Regardless of the mechanism, decreased phosphorylation of MLC may be an additional way for TPC1 to regulate cytokinesis.

TPC1 and TPC2 were recently found to form an endolysosomal channel complex with the mammalian target of rapamycin (mTOR), a complex that detects nutrient status, coupling the cell's metabolic state to endolysosomal function.[22] One potential role for the channel in controlling lysosomal membrane potential and pH is the regulation of autophagosome-lysosome fusion, one of the last steps of macroautophagy, during which nutrients such as amino acids can be generated in response to starvation.[50] In macroautophagy, portions of cytoplasm are sequestered into autophagosomes and degraded by hydrolytic enzymes following fusion of autophagosomes with the lysosomes. This process releases the breakdown products as nutrients that can be reused by the cell or exported for use by other cells.[51] Interestingly, mTOR is central in regulating the balance between autophagy and cell growth,[51] and tpc1/tpc2 double knockout mice showed defects in autophagy.[22] Autophagy was also recently shown to play a critical role in the degradation of active RhoA, with implications for cytokinesis control and genomic stability.[52] Defects in autophagy specifically drove cytokinesis failure, multinucleation and aneuploidy in correlation with the failure of RhoA to localize at the midbody, accumulating in autolysosomes instead.[52] Furthermore, constitutively active RhoA was found to inhibit proliferation by retarding cell cycle progression and impairing cytokinesis.[48] Thus, it is possible that TPC1 contributes to cytokinesis control by regulating RhoA recycling via lysosomal autophagy. Endolysosomal involvement in cytokinesis has been previously demonstrated; both copine A, a calcium-dependent membrane binding protein involved in endolysosomal membrane trafficking,[53] and clathrin-mediated membrane trafficking and processing of proteins are required for cytokinesis in Dictyostelium.[54] Endosomal sorting complex required for transport (ESCRT) components, originally found to be involved in endosomal sorting and multivesicular endosome biogenesis, have also been identified in cytokinesis control.[55]
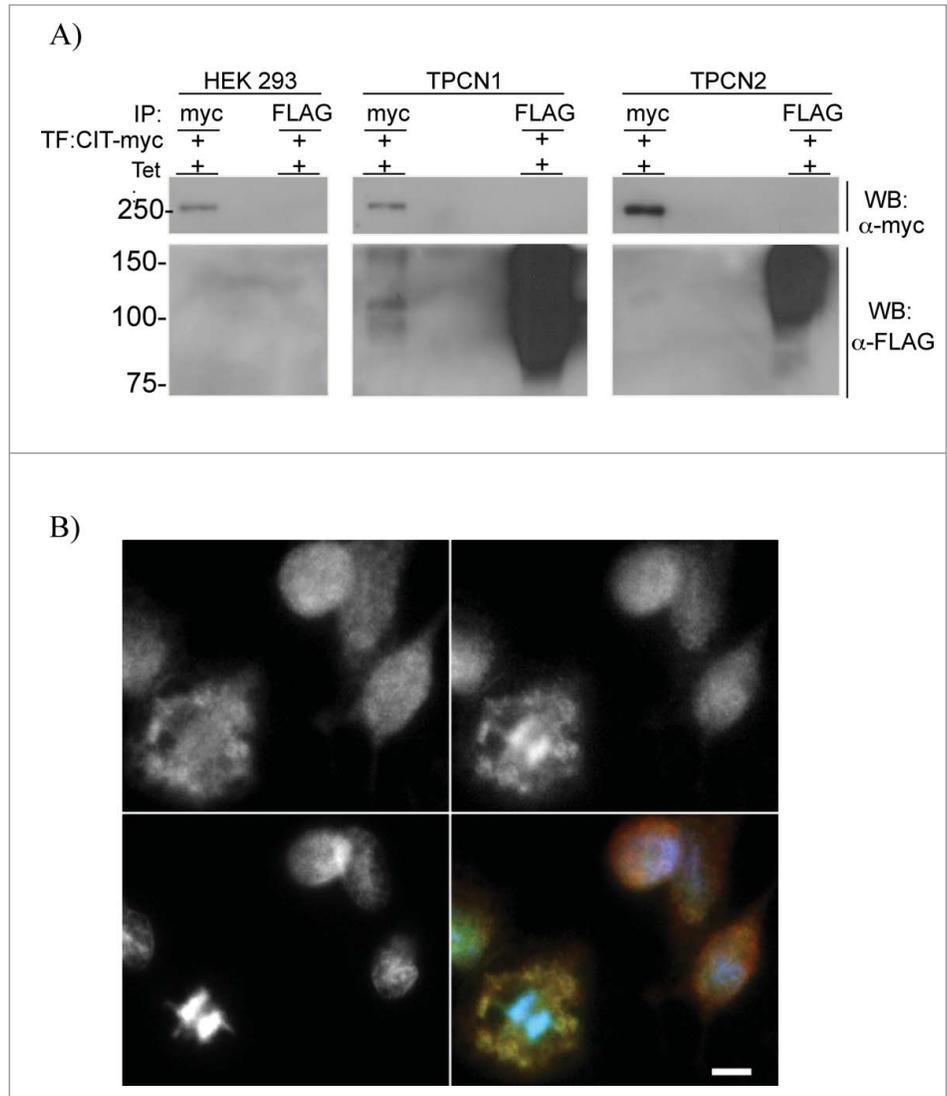
Figure 3. TPC1-CIT interaction and localization. (**A**) Co-immunoprecipitation of TPC1 and CIT-myc. HEK 293 T-REx, TPC1 and TPC2-overexpressing cells were transiently transfected with pCAG vector containing human CIT-myc. Cells were treated with tetracycline, immunoprecipitated with anti-FLAG or anti-myc antibodies and captured onto protein A agarose beads. Samples were resolved by 10% SDS-PAGE and Western blotted for anti-FLAG or anti-myc reactive proteins. TPC1-FLAG, 94 kDa; TPC2-FLAG, 85 kDa; CIT-myc, 231 kDa. (**B**) Representative fluorescence microscopy image of WT HEK 293 T-REx immunostained for endogenous TPC1 (top left panel, red channel), CIT (top right panel, green channel), DNA (bottom left panel, blue channel), and overlay (bottom right panel). Scale bar = 10 μm.

Abscission is known to be carried out by the combination of several events including vesicle trafficking, microtubule remodeling and membrane deformation.[56-58]

Cytokinesis failure leads to centrosome amplification and production of tetraploid cells, introducing chromosomal instability and setting the stage for tumor cell development.[23,32] Expression of TPC1 was significantly upregulated in a human protein array of tumor tissue compared to normal tissue, suggesting that dysregulated TPC1 expression may contribute to the aberrant cell division prominent in many cancers. Furthermore, CIT is frequently upregulated in hepatocellular carcinoma,[37] further highlighting the role of abscission control in carcinogenesis.
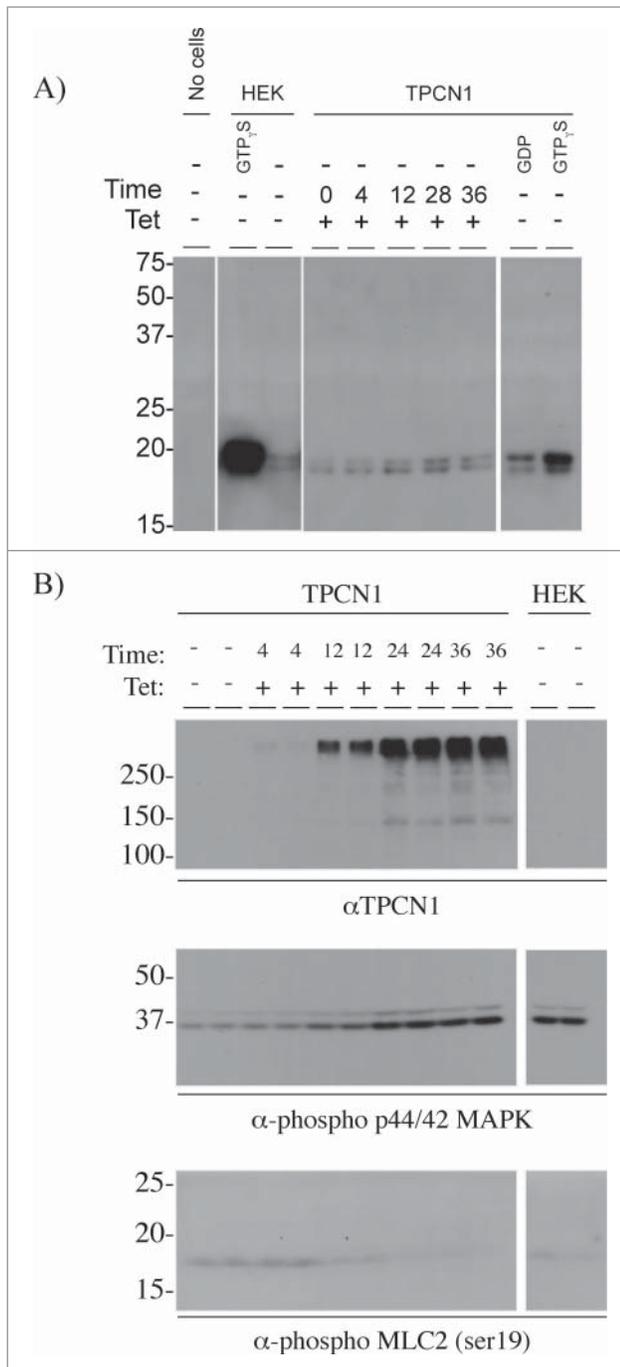
Figure 4. Effects of TPC1 overexpression on cytokinesis signaling. (**A**) Levels of active RhoGTP in cells overexpressing TPC1. Cells were treated with vehicle or induced with tetracycline, lysed, and incubated with 10 mM EDTA containing 100 μM GTPγS or 1 mM GDP. Active RhoGTP was captured onto rhotekin-RBD agarose beads and resolved by 10% SDS-PAGE and Western blotted for anti-Rho reactive proteins. (**B**) Levels of phospho-p44/42 MAPK and pMLC in TPC1-overexpressing cells. TPC1 expression was induced with tetracycline over 36 h. Cell lysates were acetone precipitated, normalized by protein concentration, and resolved by 10% SDS-PAGE and Western blotted for TPC1, phospho-p44/42 MAPK and pMLC2 (ser19) reactive proteins.

	1 & 2	3 & 4	5 & 6	7 & 8	9 & 10	11 & 12	13 & 14	15 & 16
A	Positive Control	Negative Control	Adrenal Tumor	Normal Adrenal	Bladder Tumor	Normal Bladder	Bone Tumor	Normal Bone
B	Brain Tumor Astrocytoma	Normal Brain	Brain Tumor Astrocytoma	Normal Brain	Brain Tumor Glioblastoma	Normal Brain	Brain Tumor Neuroepithelioma	Normal Brain
C	Breast Tumor Invasive Ductal Carcinoma	Normal Breast	Breast Tumor Invasive Ductal Carcinoma	Normal Breast	Breast Tumor Invasive Ductal Carcinoma	Normal Breast	Breast Tumor Invasive Ductal Carcinoma	Normal Breast
D	Colon tumor Adenocarcinoma	Normal Colon	Colon Tumor Adenocarcinoma	Normal Colon	Duodenum Tumor Adenocarcinoma	Normal Duodenum	Esophagus Tumor Squamous Cell Carcinoma	Normal Esophagus
E	Kidney Tumor Clear Cell Carcinoma	Normal Kidney	Kidney Tumor Granular Cell Carcinoma	Normal Kidney	Liver Tumor Adenocarcinoma	Normal Liver	Liver Tumor Cholangiocellular Carcinoma	Normal Liver
F	Liver Tumor Hepatocellular Carcinoma	Normal Liver	Lung Tumor Adenocarcinoma	Normal Lung	Lung Tumor Adenocarcinoma	Normal Lung	Lung Tumor Squamous Cell Carcinoma	Normal Lung
G	Lung Tumor Squamous cell Carcinoma	Normal Lung	Lung Tumor Squamous Cell Carcinoma	Normal Lung	Lymphoma	Normal Lymph Node	Ovary Tumor Clear Cell Carcinoma	Normal Ovary
H	Ovary Tumor Granular Cell Carcinoma	Normal Ovary	Ovary Tumor Thecoma	Normal Ovary	Pancreas Tumor Adenocarcinoma	Normal Pancreas	Pancrease Tumor Adenocarcinoma	Normal Pancreas
I	Pancreas Tumor Adenocarcinoma	Normal Pancreas	Parotid Tumor	Normal Parotid	Prostate Tumor	Normal Prostate	Rectum Adenocarcinoma	Normal Rectum
J	Rectum Adenocarcinoma	Normal Rectum	Skin Tumor	Normal Skin	Small Intestine Tumor Leiomyoma	Normal Small Intestine	Small Intestine Tumor Non-Hodgekin's Lymphoma	Normal Small Intestine
K	Stomach Tumor Adeno-squamous Cell Carcinoma	Normal Stomach	Testis Tumor	Normal Testis	Thymus Tumor Malignant Thymoma	Normal Thymus	ThymusTumor Thymoma (mixed)	Normal Thymus
L	Thyroid Tumor	Normal Thyroid	Ureter Tumor	Normal Ureter	Uterus Tumor Endometrium Adenocarcinoma	Normal Uterus	Uterus Tumor Endometrium Adenocarcinoma	Normal Uterus

Figure 5. TPC1 expression in human tumor tissue samples. (**A**) Western blot analysis of TPC1 expression in a human protein array of tumor and normal tissues (Biochain). Protein array was probed with anti-TPC1 (1 ug/ml) and visualized by ECL Plus (GE Healthcare) chemiluminescence detection reagent. (**B**) Box plots showing the overall range of TPC1 expression in normal vs. tumor tissue. Scores are as follows: top 25% quartiles (top whiskers), middle/median quartile (box), median (notch), bottom 25% quartile (lower whiskers), outliers (dots). *P*-value = 0.032.

Endogenous protein levels of TPC1 appear to be carefully orchestrated during cell cycle progression, with greatest expression at G2/M. In this study, we have induced TPC1 overexpression in HEK 293TREX cells, disrupting this critical balance, and causing multinucleation and cessation of complete cytokinesis. Consistent with these findings, TPC1 expression was increased in tumor tissues, implicating a new role for TPC1 in tumor progression. We also identified the major abscission control kinase CIT as a novel binding partner of TPC1. While gain-of-function experiments do pose a limitation in interpreting normal WT
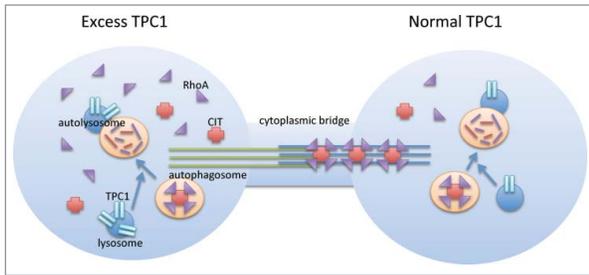
Figure 6. Proposed model of TPC1 involvement in cytokinesis. TPC1 overexpression causes an imbalance in autophagy, dysregulation of spatial and/or temporal localization of CIT, affecting proper RhoA localization at the midbody and abscission failure. In WT cells with tightly controlled TPC1 expression, TPC1 likely helps to maintain RhoA homeostasis through normal turnover via lysosomal autophagy. The scaffold protein CIT directs RhoA localization to the midbody for abscission and cytokinesis completion.

function, it is probable that TPC1 overexpression causes dysregulation of spatial and/or temporal localization of CIT, affecting proper RhoA localization and abscission function. Thus, in WT cells, TPC1 likely regulates active RhoA homeostasis, through lysosomal autophagy, via the scaffold protein CIT (**Fig. 6**). While other signaling mechanisms of this process remain to be verified, the involvement of the endolysosomal system in cytokinesis completion has been established, highlighting a central role for the phosphoinositide-activated sodium-selective TPC1 ion channel.

References

1. Yu FH, Catterall WA. The VGL-chanome: a protein superfamily specialized for electrical signaling and ionic homeostasis. Sci STKE 2004; 2004:re15; PMID:15467096

2. Ishibashi K, Suzuki M, Imai M. Molecular cloning of a novel form (two-repeat) protein related to voltage-gated sodium and calcium channels. Biochem Biophys Res Commun 2000; 270:370-6; PMID:10753632; http://dx.doi.org/10.1006/bbrc.2000.2435

3. Calcraft PJ, Ruas M, Pan Z, Cheng X, Arredouani A, Hao X, Tang J, Rietdorf K, Teboul L, Chuang KT, et al. NAADP mobilizes calcium from acidic organelles through two-pore channels. Nature 2009; 459:596-600; PMID:19387438; http://dx.doi.org/10.1038/nature08030

4. Brailoiu E, Churamani D, Cai X, Schrlau MG, Brailoiu GC, Gao X, Hooper R, Boulware MJ, Dun NJ, Marchant JS, et al. Essential requirement for two-pore channel 1 in NAADP-mediated calcium signaling. J Cell Biol 2009; 186:201-9; PMID:19620632; http://dx.doi.org/10.1083/jcb.200904073

5. Cai X, Patel S. Degeneration of an intracellular ion channel in the primate lineage by relaxation of selective constraints. Mol Biol Evol 2010; 27:2352-9; PMID:20463046; http://dx.doi.org/10.1093/molbev/msq122

6. Zong X, Schieder M, Cuny H, Fenske S, Gruner C, Rotzer K, Griesbeck O, Harz H, Biel M, Wahl-Schott C. The two-pore channel TPCN2 mediates NAADP-dependent Ca(2+)-release from lysosomal stores. Pflugers Arch 2009; 458:891-9; PMID:19557428

7. Ruas M, Rietdorf K, Arredouani A, Davis LC, Lloyd-Evans E, Koegel H, Funnell TM, Morgan AJ, Ward JA, Watanabe K, et al. Purified TPC isoforms form NAADP receptors with distinct roles for Ca(2+) signaling and endolysosomal trafficking. Curr Biol 2010; 20:703-9; PMID:20346675

8. Furuichi T, Cunningham KW, Muto S. A putative two pore channel AtTPC1 mediates Ca(2+) flux in Arabidopsis leaf cells. Plant Cell Physiol 2001; 42:900-5; PMID:11577183

9. Peiter E, Maathuis FJ, Mills LN, Knight H, Pelloux J, Hetherington AM, Sanders D. The vacuolar Ca^{2+}-activated channel TPC1 regulates germination and stomatal movement. Nature 2005; 434:404-8; PMID:15772667; http://dx.doi.org/10.1038/nature03381

10. Pottosin, II, Schonknecht G. Vacuolar calcium channels. J Exp Bot 2007; 58:1559-69; PMID:17355948; http://dx.doi.org/10.1093/jxb/erm035

11. Aley PK, Mikolajczyk AM, Munz B, Churchill GC, Galione A, Berger F. Nicotinic acid adenine dinucleotide phosphate regulates skeletal muscle differentiation via action at two-pore channels. Proc Natl Acad Sci U S A 2010; 107:19927-32; PMID:21041635; http://dx.doi.org/10.1073/pnas.1007381107

12. Tugba Durlu-Kandilci N, Ruas M, Chuang KT, Brading A, Parrington J, Galione A. TPC2 proteins mediate nicotinic acid adenine dinucleotide phosphate (NAADP)- and agonist-evoked contractions of smooth muscle. J Biol Chem 2010; 285:24925-32; PMID:20547763; http://dx.doi.org/10.1074/jbc.M110.129833

13. Esposito B, Gambara G, Lewis AM, Palombi F, D'Alessio A, Taylor LX, Genazzani AA, Ziparo E, Galione A, Churchill GC, et al. NAADP links histamine H1 receptors to secretion of von Willebrand factor in human endothelial cells. Blood 2011; 117:4968-77; PMID:21364192; http://dx.doi.org/10.1182/blood-2010-02-266338

14. Brailoiu E, Churamani D, Pandey V, Brailoiu GC, Tuluc F, Patel S, Dun NJ. Messenger-specific role for nicotinic acid adenine dinucleotide phosphate in neuronal differentiation. J Biol Chem 2006; 281:15923-8; PMID:16595650; http://dx.doi.org/10.1074/jbc.M602249200

15. Boittin FX, Dipp M, Kinnear NP, Galione A, Evans AM. Vasodilation by the calcium-mobilizing messenger cyclic ADP-ribose. J Biol Chem 2003; 278:9602-8; PMID:12486132; http://dx.doi.org/10.1074/jbc.M204891200

16. Brailoiu GC, Gurzu B, Gao X, Parkesh R, Aley PK, Trifa DI, Galione A, Dun NJ, Madesh M, Patel S, et al. Acidic NAADP-sensitive calcium stores in the endothelium: agonist-specific recruitment and role in regulating blood pressure. J Biol Chem 2010; 285:37133-7; PMID:20876534; http://dx.doi.org/10.1074/jbc.C110.169763

17. Davis LC, Morgan AJ, Chen JL, Snead CM, Bloor-Young D, Shenderov E, Stanton-Humphreys MN, Conway SJ, Churchill GC, Parrington J, et al. NAADP activates two-pore channels on T cell cytolytic granules to stimulate exocytosis and killing. Cur Biol 2012; 22:2331-7; PMID:23177477

18. Pitt SJ, Lam AK, Rietdorf K, Galione A, Sitsapesan R. Reconstituted human TPC1 is a proton-permeable ion channel and is activated by NAADP or Ca^{2+}. Sci Signal 2014; 7:ra46; PMID:24847115; http://dx.doi.org/10.1126/scisignal.2004854

19. Lin-Moshier Y, Walseth TF, Churamani D, Davidson SM, Slama JT, Hooper R, Brailoiu E, Patel S, Marchant JS. Photoaffinity labeling of nicotinic acid adenine dinucleotide phosphate (NAADP) targets in mammalian cells. J Biol Chem 2012; 287:2296-307; PMID:22117075; http://dx.doi.org/10.1074/jbc.M111.305813

20. Walseth TF, Lin-Moshier Y, Jain P, Ruas M, Parrington J, Galione A, Marchant JS, Slama JT. Photoaffinity labeling of high affinity nicotinic acid adenine dinucleotide phosphate (NAADP)-binding proteins in sea urchin egg. J Biol Chem 2012; 287:2308-15; PMID:22117077; http://dx.doi.org/10.1074/jbc.M111.306563

21. Wang X, Zhang X, Dong XP, Samie M, Li X, Cheng X, Goschka A, Shen D, Zhou Y, Harlow J, et al. TPC proteins are phosphoinositide- activated sodium-selective ion channels in endosomes and lysosomes. Cell 2012; 151:372-83; PMID:23063126; http://dx.doi.org/10.1016/j.cell.2012.08.036

22. Cang C, Zhou Y, Navarro B, Seo YJ, Aranda K, Shi L, Battaglia-Hsu S, Nissim I, Clapham DE, Ren D. mTOR regulates lysosomal ATP-sensitive two-pore Na (+) channels to adapt to metabolic state. Cell 2013; 152:778-90; PMID:23394946; http://dx.doi.org/10.1016/j.cell.2013.01.023

23. Normand G, King RW. Understanding cytokinesis failure. Adv Exp Med Biol 2010; 676:27-55; PMID:20687468; http://dx.doi.org/10.1007/978-1-4419-6199-0_3

24. Hognas G, Hamalisto S, Rilla K, Laine JO, Vilkki V, Murumagi A, Edgren H, Kallioniemi O, Ivaska J. Aneuploidy facilitates oncogenic transformation via specific genetic alterations, including Twist2 upregulation. Carcinogenesis 2013; 34:2000-9; PMID:23689353; http://dx.doi.org/10.1093/carcin/bgt171

25. Lv L, Zhang T, Yi Q, Huang Y, Wang Z, Hou H, Zhang H, Zheng W, Hao Q, Guo Z, Cooke HJ, Shi Q. Tetraploid cells from cytokinesis failure induce aneuploidy and spontaneous transformation of mouse ovarian surface epithelial cells. Cell cycle 2012; 11:2864-75; PMID:22801546; http://dx.doi.org/10.4161/cc.21196

26. Fujiwara T, Bandi M, Nitta M, Ivanova EV, Bronson RT, Pellman D. Cytokinesis failure generating tetraploids promotes tumorigenesis in p53-null cells. Nature 2005; 437:1043-7; PMID:16222300; http://dx.doi.org/10.1038/nature04217

27. Bassi ZI, Audusseau M, Riparbelli MG, Callaini G, D'Avino PP. Citron kinase controls a molecular network required for midbody formation in cytokinesis. Proc Natl Acad Sci U S A 2013; 110:9782-7; PMID:23716662; http://dx.doi.org/10.1073/pnas.1301328110

28. Piekny A, Werner M, Glotzer M. Cytokinesis: welcome to the Rho zone. Trends Cell Biol 2005; 15:651-8; PMID:16243528; http://dx.doi.org/10.1016/j.tcb.2005.10.006

29. Werner M, Glotzer M. Control of cortical contractility during cytokinesis. Biochem Soc Trans 2008; 36:371-7; PMID:18481961; http://dx.doi.org/10.1042/BST0360371

30. Gai M, Camera P, Dema A, Bianchi F, Berto G, Scarpa E, Germena G, Di Cunto F. Citron kinase controls abscission through RhoA and anillin. Mol Biol Cell 2011; 22:3768-78; PMID:21849473; http://dx.doi.org/10.1091/mbc.E10-12-0952

31. Bassi ZI, Verbrugghe KJ, Capalbo L, Gregory S, Montembault E, Glover DM, D'Avino PP. Sticky/Citron kinase maintains proper RhoA localization at the cleavage site during cytokinesis. J Cell Biol 2011; 195:595-603; PMID:22084308; http://dx.doi.org/10.1083/jcb.201105136

32. Ganem NJ, Storchova Z, Pellman D. Tetraploidy, aneuploidy and cancer. Curr Opin Genet Dev 2007; 17:157-62; PMID:17324569

33. Di Cunto F, Imarisio S, Hirsch E, Broccoli V, Bulfone A, Migheli A, Atzori C, Turco E, Triolo R, Dotto GP, et al. Defective neurogenesis in citron kinase knockout mice by altered cytokinesis and massive apoptosis. Neuron 2000; 28:115-27; PMID:11086988; http://dx.doi.org/10.1016/S0896-6273(00)00090-8

34. Cunto FD, Imarisio S, Camera P, Boitani C, Altruda F, Silengo L. Essential role of citron kinase in cytokinesis of spermatogenic precursors. J Cell Sci 2002; 115:4819-26; PMID:12432070; http://dx.doi.org/10.1242/jcs.00163

35. Liu H, Di Cunto F, Imarisio S, Reid LM. Citron kinase is a cell cycle-dependent, nuclear protein required for G2/M transition of hepatocytes. J Biol Chem 2003; 278:2541-8; PMID:12411428; http://dx.doi.org/10.1074/jbc.M210391200

36. D'Avino PP, Savoian MS, Glover DM. Mutations in sticky lead to defective organization of the contractile ring during cytokinesis and are enhanced by Rho and suppressed by Rac. J Cell Biol 2004; 166:61-71; PMID:15240570; http://dx.doi.org/10.1083/jcb.200402157

37. Fu Y, Huang J, Wang KS, Zhang X, Han ZG. RNA interference targeting CITRON can significantly inhibit the proliferation of hepatocellular carcinoma cells. Mol Biol Rep 2011; 38:693-702; PMID:20369383; http://dx.doi.org/10.1007/s11033-010-0156-5

38. Eda M, Yonemura S, Kato T, Watanabe N, Ishizaki T, Madaule P, Narumiya S. Rho-dependent transfer of Citron-kinase to the cleavage furrow of dividing cells. J Cell Sci 2001; 114:3273-84; PMID:11591816

39. Yamashiro S, Totsukawa G, Yamakita Y, Sasaki Y, Madaule P, Ishizaki T, Narumiya S, Matsumura F. Citron kinase, a Rho-dependent kinase, induces di-phosphorylation of regulatory light chain of myosin II. Mol Biol Cell 2003; 14:1745-56; PMID:12802051; http://dx.doi.org/10.1091/mbc.E02-07-0427

40. Matsumura F. Regulation of myosin II during cytokinesis in higher eukaryotes. Trends Cell Biol 2005; 15:371-7; PMID:15935670; http://dx.doi.org/10.1016/j.tcb.2005.05.004

41. Gruneberg U, Neef R, Li X, Chan EH, Chalamalasetty RB, Nigg EA, Barr FA. KIF14 and citron kinase act together to promote efficient cytokinesis. J Cell Biol 2006; 172:363-72; PMID:16431929; http://dx.doi.org/10.1083/jcb.200511061

42. Neumann B, Walter T, Heriche JK, Bulkescher J, Erfle H, Conrad C, Rogers P, Poser I, Held M, Liebel U, et al. Phenotypic profiling of the human genome by time-lapse microscopy reveals cell division genes. Nature 2010; 464:721-7; PMID:20360735; http://dx.doi.org/10.1038/nature08869

43. Serres MP, Kossatz U, Chi Y, Roberts JM, Malek NP, Besson A. p27(Kip1) controls cytokinesis via the regulation of citron kinase activation. J Clin Invest 2012; 122:844-58; PMID:22293177; http://dx.doi.org/10.1172/JCI60376

44. Chang Y, Klezovitch O, Walikonis RS, Vasioukhin V, LoTurco JJ. Discs large 5 is required for polarization of citron kinase in mitotic neural precursors. Cell Cycle 2010; 9:1990-7; PMID:20436275; http://dx.doi.org/10.4161/cc.9.10.11730

45. Camera P, da Silva JS, Griffiths G, Giuffrida MG, Ferrara L, Schubert V, Imarisio S, Silengo L, Dotti CG, Di Cunto F. Citron-N is a neuronal Rho-associated protein involved in Golgi organization through actin cytoskeleton regulation. Nat Cell Biol 2003; 5:1071-8; PMID:14595335; http://dx.doi.org/10.1038/ncb1064

46. Chang Y, Paramasivam M, Girgenti MJ, Walikonis RS, Bianchi E, LoTurco JJ. RanBPM regulates the progression of neuronal precursors through M-phase at the surface of the neocortical ventricular zone. Dev Neurobiol 2010; 70:1-15; PMID:19790105

47. Lowery DM, Clauser KR, Hjerrild M, Lim D, Alexander J, Kishi K, Ong SE, Gammeltoft S, Carr SA, Yaffe MB. Proteomic screen defines the Polo-box domain interactome and identifies Rock2 as a Plk1 substrate. EMBO J 2007; 26:2262-73; PMID:17446864; http://dx.doi.org/10.1038/sj.emboj.7601683

48. Morin P, Flors C, Olson MF. Constitutively active RhoA inhibits proliferation by retarding G(1) to S phase cell cycle progression and impairing cytokinesis. Eur J Cell Biol 2009; 88:495-507; PMID:19515453; http://dx.doi.org/10.1016/j.ejcb.2009.04.005

49. Dean SO, Spudich JA. Rho kinase's role in myosin recruitment to the equatorial cortex of mitotic Drosophila S2 cells is for myosin regulatory light chain phosphorylation. PloS One 2006; 1:e131; PMID:17205135; http://dx.doi.org/10.1371/journal.pone.0000131

50. Mizushima N, Komatsu M. Autophagy: renovation of cells and tissues. Cell 2011; 147:728-41; PMID:22078875; http://dx.doi.org/10.1016/j.cell.2011.10.026

51. Neufeld TP. Autophagy and cell growth–the yin and yang of nutrient responses. J Cell Sci 2012; 125:2359-68; PMID:22649254; http://dx.doi.org/10.1242/jcs.103333

52. Belaid A, Cerezo M, Chargui A, Corcelle-Termeau E, Pedeutour F, Giuliano S, Ilie M, Rubera I, Tauc M, Barale S, et al. Autophagy plays a critical role in the degradation of active RHOA, the control of cell cytokinesis, and genomic stability. Cancer Res 2013; 73:4311-22; PMID:23704209; http://dx.doi.org/10.1158/0008-5472.CAN-12-4142

53. Damer CK, Bayeva M, Kim PS, Ho LK, Eberhardt ES, Socec CI, Lee JS, Bruce EA, Goldman-Yassen AE, Naliboff LC. Copine A is required for cytokinesis, contractile vacuole function, and development in Dictyostelium. Eukaryotic Cell 2007; 6:430-42; PMID:17259548; http://dx.doi.org/10.1128/EC.00322-06

54. Niswonger ML, O'Halloran TJ. A novel role for clathrin in cytokinesis. Proc Natl Acad Sci U S A 1997; 94:8575-8; PMID:9238018; http://dx.doi.org/10.1073/pnas.94.16.8575

55. Rusten TE, Vaccari T, Stenmark H. Shaping development with ESCRTs. Nat Cell Biol 2012; 14:38-45; http://dx.doi.org/10.1038/ncb2381

56. Barr FA, Gruneberg U. Cytokinesis: placing and making the final cut. Cell 2007; 131:847-60; PMID:18045532; http://dx.doi.org/10.1016/j.cell.2007.11.011

57. Steigemann P, Gerlich DW. Cytokinetic abscission: cellular dynamics at the midbody. Trends Cell Biol 2009; 19:606-16; PMID:19733077; http://dx.doi.org/10.1016/j.tcb.2009.07.008

58. Neto H, Gould GW. The regulation of abscission by multi-protein complexes. J Cell Sci 2011; 124:3199-207; PMID:21940792; http://dx.doi.org/10.1242/jcs.083949